Research Article

For reprint orders, please contact: reprints@futuremedicine.com

Nanomedicine

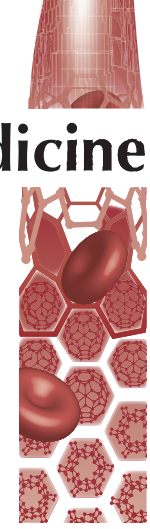

Development of upconversion nanoparticle-conjugated indium phosphide quantum dot for matrix metalloproteinase-2 cancer transformation sensing

Ming-Hsien Chan[†,‡,1,2], Chen-Yu Lai[‡,3], Yung-Chieh Chan[4], Michael Hsiao[*,4,5], Ren-Jei Chung[**,3], Xueyuan Chen[2] & Ru-Shi Liu[***,1,4,6]

[1]Department of Chemistry, National Taiwan University, Taipei 106, Taiwan

[2]CAS Key Laboratory of Design & Assembly of Functional Nanostructures, & Fujian Key Laboratory of Nano-materials, Fujian Institute of Research on the Structure of Matter, Chinese Academy of Sciences, Fuzhou, Fujian 350002, PR China

[3]Department of Chemical Engineering & Biotechnology, National Taipei University of Technology, Taipei 106, Taiwan

[4]Genomics Research Center, Academia Sinica, Taipei 115, Taiwan

[5]Department of Biochemistry College of Medicine, Kaohsiung Medical University, Kaohsiung, 807, Taiwan

[6]Department of Mechanical Engineering & Graduate, Institute of Manufacturing Technology, National Taipei University of Technology, Taipei 106, Taiwan

*Author for correspondence: mhsiao@gate.sinica.edu.tw

**Author for correspondence: rjchung@ntut.edu.tw

***Author for correspondence: rsliu@ntu.edu.tw

[†]Ming-Hsien Chan is now working at the Genomics Research Center, Academia Sinica. This research was his past Ph.D. research at the National Taiwan University.

[‡]Authors contributed equally

Aim: Matrix metalloproteinase-2 (MMP2) plays an important role in extracellular matrix remodeling, that is, it increases significantly during cancer progression. In this regard, MMP2 monitoring is important. **Experiment:** A well-designed MMP2-sensitive polypeptide chain was used to link indium phosphide quantum dots (InP QDs) with upconversion nanoparticles (UCNPs) to form a nanocomposite that was utilized as biosensor. **Results:** We produced a biosensor that can be recognized by MMP2 and determined the presence or absence of MMP2 in cells by identifying difference in fluorescence wavelength. The InP QDs modified the arginylglycylaspartic acid molecules as targeting ligand based on chitosan. **Conclusion:** The MMP2-based biosensor, named UCNP-p@InP-cRGD, is sensitive and can be applied for biosensing probes.

Graphical abstract:

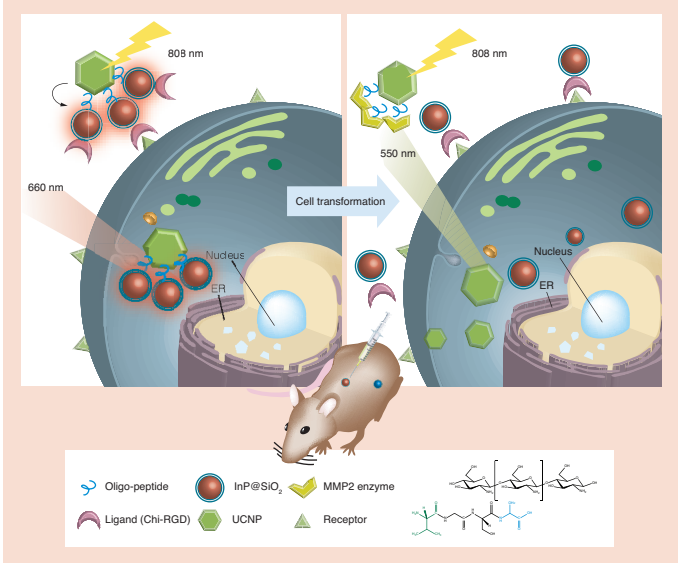

Future Medicine

First draft submitted: 31 December 2018; Accepted for publication: 2 April 2019; Published online: 15 July 2019

Keywords: bio-conjugating • indium phosphide quantum dots • MMP2 sensing • Nd^{3+}-sensitized upconversion nanoparticles • targeting

Quantum dots (QDs) are nanocrystalline semiconductor materials. QDs of different particle sizes can be excited to emit different colors of fluorescence because of the effects of quantum confinement [1]. Compared with traditional organic dye, QDs have optical advantages, such as higher quantum field, better light stability and applicability of single-wavelength ultraviolet (UV) or visible light as source to illuminate different light wavelengths. Moreover, QDs can be repeatedly excited. At present, market-based QDs contain cadmium (Cd) [2]. However, Cd-containing QDs and their compounds are not environment friendly, which limits their biological development. Thus, a new generation of QDs without Cd, such as indium phosphide QDs (InP QDs), has been developed. The particle size of InP QDs can be adjusted to regulate the emitting wavelength. When the size of InP QDs increases to 7 nm, they can absorb UV and green light, and emit red fluorescence. If QDs are used alone, then they can only be excited by UV or visible light. However, the optical properties of QDs should be improved given that their excitation wavelength is unsuitable [3–5]. The skin can block UV light, and deoxyhemoglobin has its highest absorption peak in the region of visible light. Therefore, InP QDs can be combined with current fluorescent upconversion nanoparticles (UCNPs) to detect cell changes by fluorescence resonance energy transfer. Upconversion fluorescence is a multiemission spectrum, which is a conversion of long-wavelength absorption to short-wavelength emission, permitting the optical process to go through from near-infrared light to visible light [6–8]. The unique optical properties of UCNPs can be used as biosensors by the shifts of the spectrum from near-infrared to visible light [9,10]. UCNPs are usually synthesized by doping rare-earth elements in host materials, such as $NaYF_4$ [11]. Yb^{3+} and Er^{3+} are typically prepared as sensitizers and activators in UCNPs to irradiate green fluorescence.

In this study, we designed an inorganic nanocomposite as biosensor. We aimed to detect the presence or absence of matrix metalloproteinase-2 (MMP2) in normal and cancer cells. Extracellular matrix remodeling becomes an important issue during cancer progression given that most malignant tumor cells can destroy matrix barriers to promote cancer cell invasion to connective tissues and metastasis to distant organs [12–14]. Collagenases can degrade fibrillar collagens when MMP overexpression has been identified to be a marker of cancer progression that involves metastasis and angiogenesis. MMP2 belongs to the gelatinase family and can degrade type IV-extracellular proteins and nonfibrillar collagens. In many cancers, MMP production may be upregulated in surrounding tissues rather than simply in the tumor [15,16]. Few biosensors have been developed for MMP2. The first biosensor uses nitrogen-doped graphene combined with gold nanoparticles to detect MMP2 by UV-electrochemical information [17]. Fluorescein isothiocyanate-labeled peptide on the surface of poly(m-phenylenediamine) nanoparticles can be designed to detect MMP2 with a limitation of 32 pM [18]. Studies only used measurement of MMP2 to *in vitro* assays. In this study, we designed an MMP2-sensing polypeptide as a linker to conjugate InP QDs and UCNPs (UCNP-p@InP). These two materials were combined to form a nanocomposite and excited with an 808 nm laser light to transfer upconverted light to InP QDs and illuminate red fluorescence for biotracking. In environments with a high concentration of MMP2, MMP2 sensing polypeptide is recognized by MMP2 and sheared to separate these two nanoparticles. Thus far, we can only observe upconverting green light under irradiation of 808 nm near-infrared light. To improve the capability of UCNP-p@InPs to effectively accumulate around the tumor tissue and enhance biosensing, we used arginylglycylaspartic acid (RGD) molecules as target ligands [19]. RGD is a well-known targeting molecule that binds to integrin $\alpha_V\beta_3$. Given the high expression of integrin $\alpha_V\beta_3$ in many types of cancer cells, RGD is used to construct multifunctional 'smart' ligands, such as tumor-targeted nanoparticles [20–22]. The accumulation of the entire material in the tumor tissue is enhanced to effectively obtain a fluorescent signal that differs from the background. Cell experiments, confocal imaging and luciferase biopsy analyses are conducted. Results prove that the nanocomposites have excellent biological targeting and tracking abilities. Upon infrared laser irradiation, near-infrared-induced MMP2 sensor demonstrates excellent applicability in animal models and clinical trials.

Materials & methods

Materials

All chemical reagents were obtained from commercial suppliers and did not require further purification. Synthetic chemicals of InP QDs are $In(C_2H_3O_2)_3$ (99.99%), $[(CH_3)_3Si]_3P$ (98%), myristic acid (98%), $CH_3(CH_2)_{11}SH$

(≥98%), $[CH_3(CH_2)_{16}COO]_2$ Zn (10%, Zn basis), oleic acid (90%), 1-octadecene (90%), n-trioctylphosphine (90%), selenium powder (99.99%), $(CH_3CO_2)_2$ Zn (99%) and hexane (99.99%). Synthetic chemicals of UCNPs are $Nd(CH_3CO_2)_3{\cdot}H_2O$ (99.99%), $Y(CH_3CO_2)_3{\cdot}H_2O$ (99.99%), $Yb(CH_3CO_2)_3{\cdot}H_2O$ (99.99%), $Er(CH_3CO_2)_3{\cdot}H_2O$ (99.99%), NaOH (98%) and HCl (37%). Chemicals used for modification are APTES (98%), IGEPAL® CO-520, tetraethyl orthosilicate (98%), N-(3-dimethylaminopropyl)-N-ethylcarbodiimide hydrochloride (EDC), N-hydroxysuccinimide (NHS), chitosan (molecular weight [mol wt.] 50,000–190,000 Da) and Arg-Gly-Asp (≥97%). All chemicals were purchased from Sigma-Aldrich (MO, USA), except $In(C_2H_3O_2)_3$. Selenium powder was purchased from Alfa Aesar (MA, USA). Myristic acid was acquired from Fluka (MO, USA), and $(CH_3CO_2)_2$ Zn was supplied by JT Baker (NJ, USA). The 4′,6-Diamidino-2-phenylindole (DAPI) and Alexa 647 were purchased from Invitrogen (CA, USA).

Synthesis of InP/ZnSeS/ZnS QDs & silica shell coating (InP@S QDs)

InP/ZnSeS/ZnS QDs were synthesized using hot injection method as previously described [23]. In total, 0.3 mmol indium acetate, 1.35 mmol myristic acid, 0.3 mmol zinc stearate and 10 ml of 1-octadecene were mixed in a three-necked flask under vacuum. The rotation speed was 450 rpm, and the temperature was increased to 120°C and maintained for 1 h to completely remove water and gas and avoid inefficient QDs. After an hour, the vacuum system was closed and nitrogen was allowed to pass through. The system was added with 0.1 mmol tris(trimethylsilyl)phosphine under nitrogen, and the temperature was increased to 260°C for 20 min to obtain InP core. The temperature was decreased to 230°C, and 0.22 ml of 1-dodecanethiol was added for 1 h. After an hour, 0.2 mmol selenium was added to the mixture. Subsequently, 1 ml of n-trioctylphosphine was mixed and vortexed to colorless liquid. The mixture was warmed to 280°C for 10 min and added with 4 ml of $Zn(OA)_2$. A total of 6.85 ml of octadecene (ODE) was mixed with 3.15 ml of oleic acid (OA) and heated to 120°C in a nitrogen atmosphere for 1 h. The mixture was then heated to 150°C after 10 min and added with 0.55 ml of dichlorodiphenyltrichloroethane (DDT). The temperature was increased to 300°C for 90 min. The reaction was completed. The mixture was cooled to room temperature and mixed with 5 ml of QDs, 5 ml of hexane and 20 ml of ethanol. The mixture was placed in a centrifuge tube and centrifuged four-times at 7800 rpm. The resulting QD product was dissolved in hexane for storage. After the end of the synthesis, we coated the silica shell and uniformly dispersed the QDs in water. First, the magnet was placed into a single-necked flask; added with 0.3 mg/ml QDs, 1 ml of CO520 and 9 ml of hexane; and placed in a drying oven at constant temperature and humidity. After an hour, tetraethoxysilane (TEOS) was injected at a rate of 0.05 ml/h by using a microsyringe. After approximately an hour, the mixture was added with 0.07 ml of ammonia water, stirred overnight, centrifuged at 12,000 rpm. for 6 min, and washed three-times. The InP@S QDs were dissolved in water for storage.

Synthesis of 808 nm-excited $NaYF_4$:Yb/Er@$NaYF_4$:Yb/Nd (UCNP)

UCNP was synthesized by high-temperature co-precipitation [24]. Among the main materials of UCNP, the main lattice material with the best light-emitting efficiency was $NaYF_4$. The crystal phase of $NaYF_4$ was divided into cubic phase (α-$NaYF_4$) and hexagonal phase (β-$NaYF_4$). UCNP of β form was selected because of its high chemical stability, low phonon energy and high light-emitting efficiency. $Y(CH_3CO_2)_3{\cdot}H_2O$ (0.4 mmol), $Yb(CH_3CO_2)_3{\cdot}H_2O$ (0.1 mmol) and $Er(CH_3CO_2)_3{\cdot}H_2O$ (0.1 mmol) were dissolved in OA and ODE (3:7; 12.5 ml) at 150°C under nitrogen for 30 min (Sigma-Aldrich). The dissolved lanthanide salts were cooled down to 50°C and stirred with methanol solution containing NH_4F (2 mmol) and NaOH (1.25 mmol) for 30 min. Methanol was removed by heating the solution to 100°C for 30 min. The solution was heated to 290°C for 2 h and cooled to room temperature. $NaYF_4$:Yb/Er nanoparticles were precipitated with absolute ethanol and recovered by centrifugation at 6000 rpm. for 10 min. The prepared nanoparticles were stored in cyclohexane. The shell layer was synthesized using the same method, except that the Yb precursors were replaced with Nd to prepare a core–shell structure. The lanthanum acetate aqueous solution comprised 2.55 ml of $Er(CH_3CO_2)_3{\cdot}H_2O$ (0.2 M), 0.17 ml of $Y(CH_3CO_2)_3{\cdot}H_2O$ (0.2 M) and 0.68 ml of $Nd(CH_3CO_2)_3{\cdot}H_2O$ (0.2 M). The section for synthesis was the same as the above. $NaYF_4$:Yb/Er@$NaYF_4$:Yb/Nd was obtained after centrifugation.

Conjugation of UCNPs, InP@S QDs & UCNP-p@InP-cRGD

The aqueous solution (0.5 ml) of $NaYF_4$:Yb/Er@$NaYF_4$:Yb/Nd nanoparticles with a concentration of 10 mg/ml was added with 0.2 ml of MMP2-sensitive polypeptide (named MH-P08, with amino acid sequence of 'SGAVR-WLLTA'), 0.24 ml of NHS and 0.024 ml of EDC to form UCNP-p. About 0.964 ml of the four compounds were

mixed in an Eppendorf tube, stirred overnight, centrifuged three-times with gravity at 12,000 rpm. for 10 min, and stored in an aqueous solution. InP@S QDs were conjugated with the RGD tripeptide with chitosan to form InP@S-cRGD. First, 1 wt% chitosan was mixed with 2 wt% aqueous acetic acid solution. An aqueous solution of acetic acid with pH of 3.6 was neutralized with NaOH (200 mg) to increase the pH to 6. Subsequently, 100 mg of RGD was placed into 10 ml of aqueous solution and added with 0.3 ml of EDC and 0.3 ml of NHS. The mixture was kept in an ice bath for 15 min. An amount of 5.2 ml of chitosan acetic acid aqueous solution was added, and 0.5 ml RGD solution was obtained to stir with 0.2 mg/ml QDs overnight. The solution was centrifuged three-times at 12,000 rpm. for 10 min and stored in a sample bottle. Last, 0.25 ml of UCNP-p solution with a concentration of 10 mg/ml was taken and conjugated with InP@S-cRGD solution with the same volume and concentration. The mixture was stirred for 2 h and centrifuged three times at 12,000 rpm. for 10 min. The final product, UCNP-p@InP-cRGD, was stored in an aqueous solution.

Identification of nanomaterials

The morphologies of UCNP series (UCNP and UCNP-p) and InP QDs series (InP QDs, InP@S and InP@S-cRGD) were determined using a JEM-2100F transmission electron microscope (TEM) with an electron gun operating at 100 keV (JEOL, Tokyo, Japan). The emission spectrum of UCNP and derivatives was characterized by photoluminescence spectrum with excitation of 808 nm.

In vitro model with cell culture & cell viability

Gingival squamous cell carcinoma (Ca922) and tongue squamous cell carcinoma (HSC4) were grown in DMEM and MEM (Invitrogen), respectively. All cell culture media were supplemented with 10% fetal bovine serum (FBS, CA, USA) and 1% penicillin–streptomycin–glutamine (GIBCO, MA, USA). All cells were incubated in a CO_2 incubator containing 5% CO_2 at 37°C. Aliquots of 2000 cells per well were inoculated in a 96-well plate for 12 h. Serial diluted concentrations of UCNP-p@InP-cRGD (1, 3, 9, 27, 83 and 250 μg/ml) were incubated in a 96-well plate. After 48 h of incubation, the AlamarBlue assay was performed according to the manufacturer's protocols (Invitrogen). The detection spectrum was set at 560/590 nm (excitation/emission).

Cell sensing imaging analysis

A total of 50,000 cells were inoculated in a 12-well plate with a coverslip for 12 s. The culture was added with 100 μg/ml UCNP-p@InP-cRGD for 12 h. The cells were then fixed with 4% paraformaldehyde. The cells on the coverslip were stained with anti-α-tubulin (1:300 in 5% bovine serum albumin/phosphate-buffered saline) and attached on the slide by using DAPI-containing mounting gel. Images were promptly captured with a Leica TCS SP5 confocal microscope (Leica, Taiwan). The Leica biosystem inverted microscope was equipped with an excitation laser source of 808 nm (Leica).

Detection of MMP2 in the *in vivo* mouse model

The animal experiments were approved by the Academia Sinica Institutional Animal Care and Utilization Committee (IACUC No. 16-05-957). In brief, 5×10^6 aliquots of Ca922 and HSC4 cells were subcutaneously injected on both opposite dorsal sides of the NOD scid gamma (NSG) mouse at 6 weeks old. After 4 weeks of tumor growth (above 60 mm^3 of tumor volume), UCNP-p@InP-cRGD (20 mg/ml) was administered on both tumors by intratumoral injection. Real-time images were obtained using *In-Vivo* Xtreme (Bruker, Germany), with an additional 808 nm infrared diode laser module (1 W). The color filters were detected at 650 nm for the red fluorescence of InP QDs and 540 nm for the green fluorescence of UCNPs. Xenograft tumors were harvested using a formalin-fixed and paraffin-embedded method.

Results

This study is divided into four parts to discuss the results (Figure 1). In the first part, InP@S-cRGD modulated the QDs with a silica shell. The Si-OH group on the surface of silica was first combined with the NH_2 group on the chitin and then connected, dehydrated and combined with the C-terminus of the side chain of the multipeptide to form the Si-cRGD group. In the second part, UCNP-MMP2 (UCNP-p), 808 nm UCNPs were assembled with the linker MMP2-sensitive peptide. In the third part, UCNP-p@InP-cRGD, the COO^- functional group was modified on MMP2 and Si-OH with NH^{2+}. When assembled with RGD, nanocomposites were obtained. In the fourth part, biological interaction, after the assembled nanocomposite absorbed 808-nm near-infrared laser light,

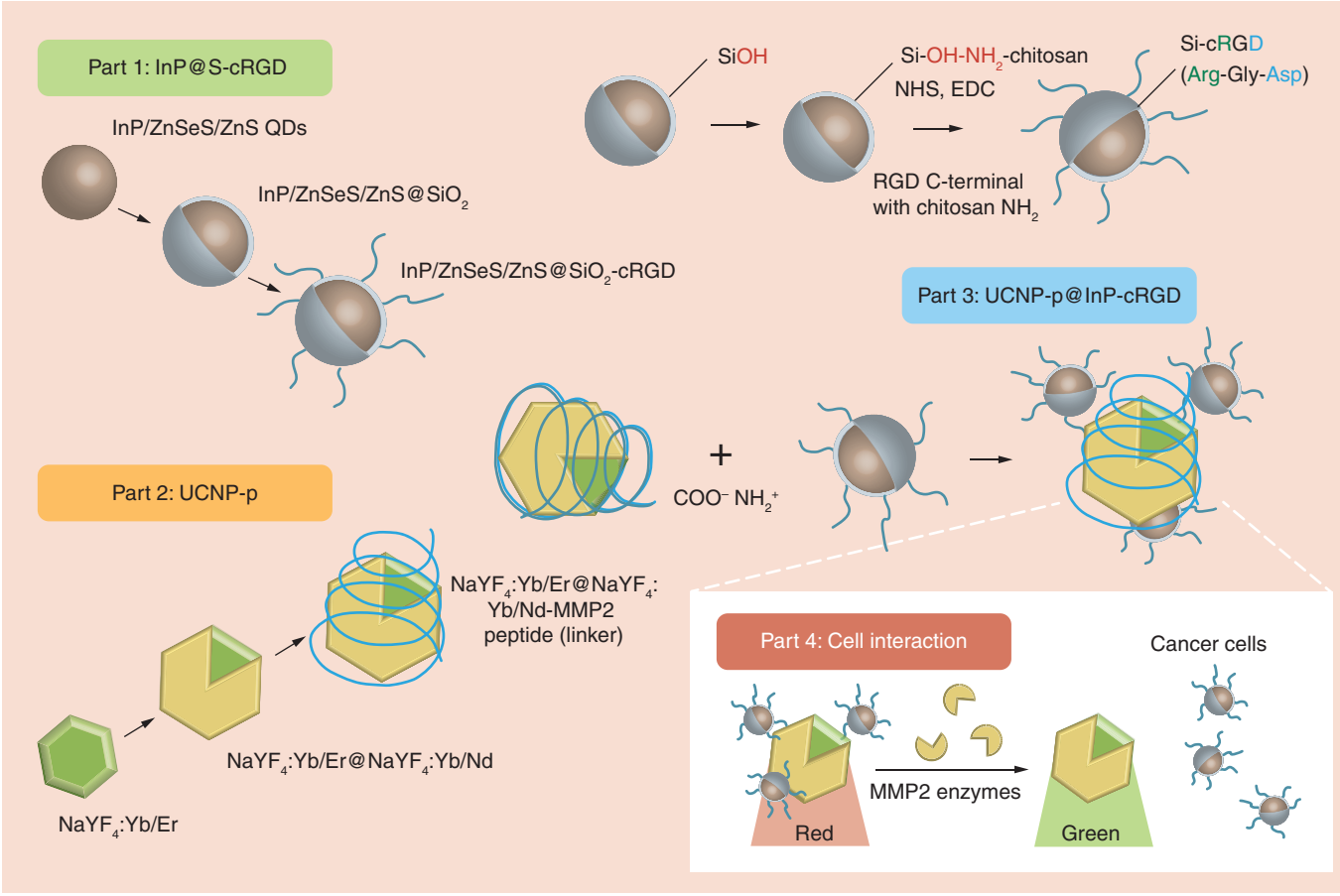

Figure 1. Upconversion nanoparticle-p@InP-cRGD sensing in an matrix metalloproteinase-2-expressed cancer cell. Upconversion nanoparticles-p@InP-cRGD was colorless under 808-nm irradiation; moreover, matrix metalloproteinase-2-digested upconversion nanoparticles underwent cell uptake and were detected using 808-nm irradiation.
InP: Indium phosphate; MMP2: Matrix metalloproteinase-2; QD: Quantum dot; UCNP: Upconversion nanoparticles.

it emitted red light of QDs. However, after cutting the nanocomposite with the MMP2 enzyme, the fluorescence phenomenon only revealed the upconverting green light. Other details of each part will be discussed below.

Synthetic identification of InP, InP@S & InP@S-cRGD

In this study, 0.3 mmol indium acetate, 0.3 mmol zinc stearate and 1.35 mmol myristic acid were used as the core precursor of InP, and phosphorus precursor and selenium were used as shell. The zinc and sulfur precursors reacted with the InP QDs of the core–shell structure, which changed the thickness of the shell layer by changing the ratio of the zinc and sulfur precursors in the shell layer and the content of the zinc stearate to regulate its core. The change in particle size will change the wavelength of light emission, and the increase in the shell thickness of the QD will increase its stability. Therefore, a thick-shelled InP QD was selected for subsequent application. This material was coated with silica shell for phase replacement and modified with tripeptide and chitosan. The silica-coated InP QD (InP@S) was characterized in terms of structural properties, biological cell compatibility and cell development. As shown in Supplementary Figure 1A, the QDs with thick shell have a regular crystal phase arrangement. The QD diameter is 7 nm based on calculated particle size. Supplementary Figure 1B shows a QD modified with a silica shell; the black particles are QDs and the outer cladding layer is made of silica. After calculation, the particle size increased from 7 to 15 nm. The identification of the hydrated particle radius size was confirmed by dynamic light scattering (DLS) analysis. As shown in Supplementary Figure 1C, the particle size of QDs, which was measured in hexane, is 9 nm. Supplementary Figure 1D shows that after the QDs were modified with the silica shell, the particle size increased from 9 to 23 nm; that is, the known QDs modified with the silica layer were successfully coated. The DLS spectrum shows that the particles are highly dispersed at 23 nm, indicating that the dispersibility in the

aqueous phase was quite good and that no aggregation occurred. After surface modification, the size distribution of InP@S-cRGD is 28 nm. The type and semiquantitative effects of internal atoms were evaluated based on the energy dispersive spectrometer (EDS) analysis.

Supplementary Figure 2A shows the estimation of In, P, Se, S, Si and Zn. The element ratio of In:P is approximately 1:1. Given the multilayer modification, the ratio of Zn and S increased than that of the core material. Furthermore, the signal of Si was determined, confirming the success of silica modification. In terms of optical characteristics, the black and red curves are the absorption points of QDs and their modified QDs with the silica shell are shown in Supplementary Figure 2B. The figure also shows the obvious characteristic curve of the QDs of the black curve, with the peak value of approximately 540 nm. Compared with the red curve modified with the silica shell, the characteristic absorption peak position is nearly the same. The only difference is that the peak tends to be inconspicuous. As shown in Supplementary Figure 2C, the emission spectrum was measured using an excitation source of 460 nm. The black curve is the emission wavelength of the red QD, with the emission position at 660 nm. The QDs were modified, but the light-emitting position was the same. We also identified the fluorescent lifetime and quantum yield for InP and InP@S (Supplementary Figure 3A & Supplementary Table 1). No difference was observed in the fluorescence lifetime of QDs before and after modification. From 30 to 28 ns, the result showed only a little effect before and after the modification. The quantum efficiency also slightly decreased after coating with the silica shell. In this study, InP and InP@S were used to identify the FTIR functional group. Supplementary Figure 4B shows Si-O-Si characteristic peaks at approximately 1500 cm^{-1}, confirming the characteristic peak of the InP QDs is the coated silica layer. To attach the actively targeted RGD peptide to the surface of the QDs, we linked InP@S and RGD through chitin as intermediate (Supplementary Figure 4A). Supplementary Figure 4B shows the characteristic absorption peak of NH_2 at approximately 2900 cm^{-1}, which originates from chitosan and RGD. A characteristic absorption peak of COO^- also appears at approximately 1500 cm^{-1}, indicating the modification of RGD. The FTIR data prove the successful assembly of the cRGD.

Synthetic identification of UCNP & UCNP-p

The core–shell structure of the UCNPs was subjected to TEM measurement, and the average diameter of $NaYF_4$:Yb/Er is approximately 25 ± 1 (Supplementary Figure 5A). After coating the second shell, the average diameter of $NaYF_4$:Yb/Er@$NaYF_4$:Yb/Nd is approximately 27 ± 1 nm and the particle size increased from 25 to 27 nm (Supplementary Figure 5B). $NaYF_4$ is a pure hexagonal phase, as confirmed by x-ray powder diffraction. Supplementary Figure 5C shows that the diffraction spectrum of UCNP has a characteristic diffraction peak, similar to the hexagonal-phase β-$NaYF_4$ database standard map (JCPDS 16-0334) [25]. In the measured x-ray diffraction pattern, the main diffraction peaks are located in the growth planes of (110), (101), (201), (300) and (211). The standard map has two main diffraction peaks corresponding to the crystal planes of (300) and (211), indicating that $NaYF_4$:Yb/Er and $NaYF_4$:Yb/Er@$NaYF_4$:Yb/Nd correspond to the same standard map. This result demonstrated that the core and core–shell UCNPs have no phase change. The 808 nm-excited UCNPs were also measured for DLS analysis (Supplementary Figure 5D). The sizes of $NaYF_4$:Yb/Er and $NaYF_4$:Yb/Er@$NaYF_4$:Yb/Nd are 32 and 75 nm, respectively. The distribution curve shows that the particles did not agglomerate. In the upconversion fluorescence process, Yb and Nd acted as sensitizers that promoted the excited state at 808 nm irradiation (Supplementary Figure 6A), of which the electrons jumped from $^2F_{7/2}$ ground state to $^2F_{5/2}$ excited state. The unstable energy was then transferred to unexcited Er. The excited state of trivalent Er released energy with fluorescence, including $^4F_{9/2} \rightarrow {}^4I_{15/2}$, $^4S_{3/2} \rightarrow {}^4I_{15/2}$, $^2H_{11/2} \rightarrow {}^4I_{15/2}$, and $^2H_{9/2} \rightarrow {}^4I_{15/2}$, with corresponding 410, 522, 540 and 662 nm, respectively (Supplementary Figure 6B).

Synthetic identification of UCNP-p@InP-cRGD

UCNP was coupled with peptides and InP QDs using the NHS/EDC method to form UCNP-p and InP-cRGD [26]. The N-terminus of peptide linkage includes a carboxyl group, protruding from the peptide linkage of UCNP@p. In total, 15 nm of InP-cRGD was conjugated to the MMP2-sensitive polypeptide to form a peptide bond and the distance between UCNP and InP is <10 nm to occur the (Figure 2A). The combination of these two nanomaterials can also be seen in Figure 2B. After the InP QDs are modified and have a Si-OH group, they became negatively charged. The negative ζ-potential (-147.36 mV) can be obtained. The aspartic acid band is slightly negatively charged; however, the chitosan is positively charged, and the bond is not charged. Given that the Si-OH group on the silica shell is negatively charged, it remained negatively charged after modification, so the green bar graph can be obtained. Furthermore, a charge of -117.9 mV is obtained. When the UCNPs are not

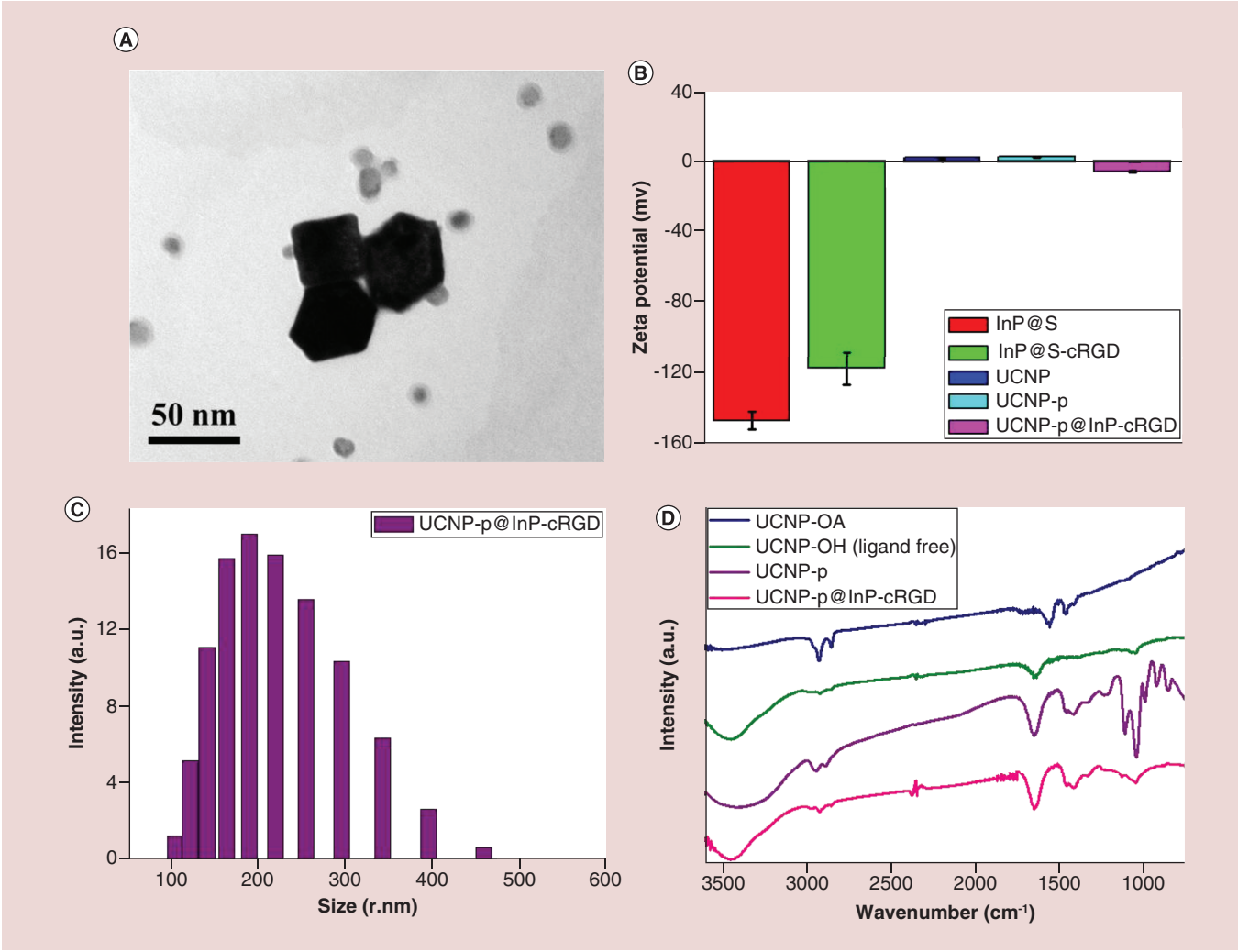

Figure 2. Basic characteristics of UCNP-p@InP-cRGD. TEM image of **(A)** upconversion nanoparticles-p@InP-cRGD. Scale bar indicated 50 nm. **(B)** Potential of nanocomposite is reached. **(C)** Size distribution of upconversion nanoparticles-p@InP-cRGD-modified matrix metalloproteinase-2. **(D)** FTIR spectra of quantum dot-modified quantum dot complexes.
cRGD: Quantum dot conjugated with the RGD tripeptide with chitosan; OA: Oleic acid; InP: Indium phosphate; InP@S: InP and silica coating quantum dot; UCNP: Upconversion nanoparticle.

charged, the dark blue bar graph with a value of 1.75 mV is obtained. The UCNPs are positively charged (2.23 mV) after being modified with the MMP2-sensitive polypeptide and the expected result is consistent. As a result, the entire nanocomposite was slightly negatively charged, and the result of the pink bar graph is -6 mV. The size distribution of this nanocomposite is around 180 nm (Figure 2C). The FTIR also indicated that the characteristic peaks appeared after the modification of both nanomaterials (Figure 2D). We identified the optical properties of UCNP-p@InP-cRGD. Figure 3A shows the overlap between the fluorescence of UCNPs and the absorption peak of InP QDs, and the phenomenon of fluorescence transfer between them. UCNP was identified as a fluorescent life cycle, and the change in its fluorescence lifetime after modification by the core–shell structure was observed. Figure 3B shows the nanocomposite of UCNPs combined with InP QDs. The lifetime was reduced from 0.58 to 0.56 ms because InP QDs absorb the upconverting fluorescence. As the characteristic peak of InP QDs absorbs the fluorescence of UCNPs, the fluorescence lifetime still has a tendency to decrease. For *in vitro* MMP2 sensing, human recombinant MMP2 was used for *in vitro* digestion of UCNP-p@InP-cRGD. The dose-dependent experiment of MMP2 digestion was performed that 20, 40, 60, 80, 100 and 120 pM human recombinant MMP2 were added into 0.2 mg/ml UCNP-p@InP-cRGD for 37°C incubation. The fluorescence intensity gradually increased with time (Figure 3C). Fluorescent emission at 540 nm demonstrated the performance of MMP2 in unraveling the

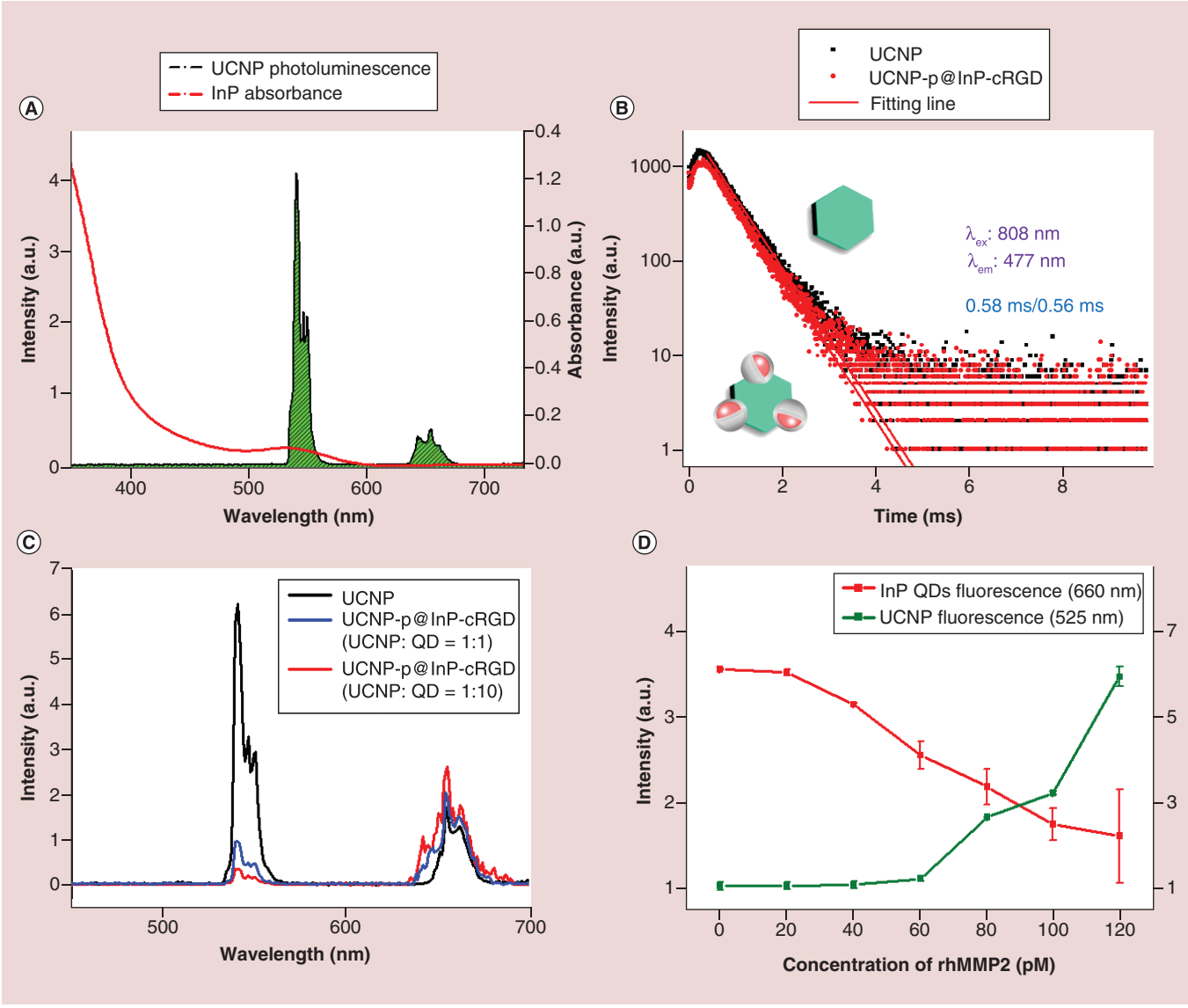

Figure 3. The optical analysis of UCNP-p@InP-cRGD. (A) Absorption and emission spectra of nanocomposites. **(B)** $NaYF_4$:Yb/Er@$NaYF_4$:Yb/Nd and $NaYF_4$:Yb/Er@$NaYF_4$:Yb/Nd-InP QD fluorescence lifetime. **(C)** Fluorescence transfer between upconversion modification and nanocomposite. **(D)** Upconversion spectra and indium phosphide quantum dot spectra with several human recombinant matrix metalloproteinase-2 proteins. The concentration-dependent digestion of matrix metalloproteinase-2 was shown using photoluminescence spectrum, wherein 0.2 mg/ml of upconversion nanoparticles-p@InP-cRGD solution was incubated with 0, 20, 40, 60, 80, 100 and 120 pg/ml of human recombinant matrix metalloproteinase-2 for 1 h.
cRGD: Quantum dot conjugated with the RGD tripeptide with chitosan; OA: Oleic acid; InP: Indium phosphate; InP@S: InP and silica coating quantum dot; UCNP: Upconversion nanoparticle.

UCNP-p@InP-cRGD. The exponential dose dependent of MMP2-digested UCNP-p@InP-cRGD was between 80 and 100 pM. All enzyme reactions reached a plateau after 1 h (Figure 3D).

In vitro cell active targeting & MMP2 sensing analysis

The cell test of UCNP-p@InP-cRGD was performed in gingival squamous cell carcinoma (Ca922) and tongue squamous cell carcinoma (HSC4). The safety of the nanocomposite is the most important factor for biological applications. The cytotoxicity of Ca922 and HSC4 was determined by AlamarBlue assay. We used different concentrations of nanocomposites incubated with Ca922 and HSC4 cell lines. After 48 h of incubation, UCNP-p@InP-cRGD showed slight cytotoxicity in Ca922 and HSC4 cell lines (Figure 4A & B). By increasing the

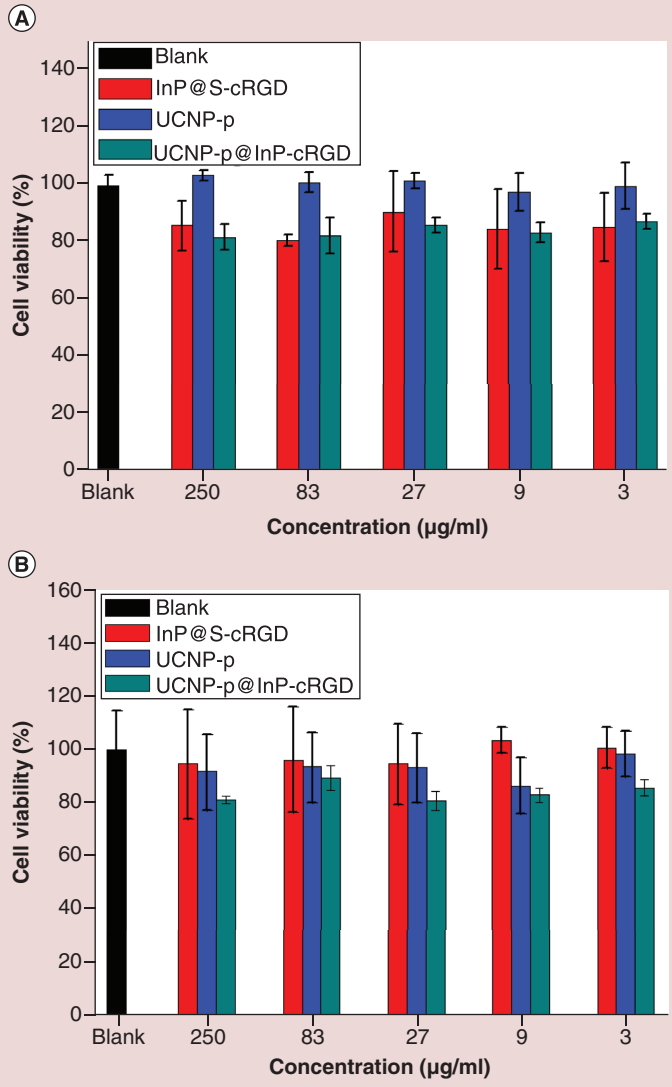

Figure 4. ***In vitro*** **cell viability test.** Cell viability assay showed upconversion nanoparticles-p@InP-cRGD incubating in the cancer cell lines of **(A)** Ca922 and **(B)** HSC4 at 24 h. Long-term incubation of upconversion nanoparticles-p@InP-cRGD was shown no toxicity in Ca922 and HSC4.
cRGD: QDs conjugated with the RGD tripeptide with chitosan; InP: Indium phosphate; InP@S: InP and silica coating quantum dot; UCNP: Upconversion nanoparticle; UCNP-p: Upconversion nanoparticle-conjugated indium phosphide quantum dot.

concentration of UCNP-p@InP-cRGD, >80% of the cells survived. To conclude the result of cell viability, UCNP-p@InP-cRGD has low cytotoxicity and is a biocompatible nanomaterial. Considering the decoration of specific MMP2-sensitive polypeptide and RGD peptide on UCNP-p@InP-cRGD, we measured the expression levels of MMP2 enzymes and integrin in these two cell lines (Figure 5). MMP2 was significantly expressed in HSC4 cell lines. In total, 10 μg/ml of UCNP-p@InP-cRGD was incubated in HSC4 cells for 12 h. After staining the nucleus with DAPI, the UCNP-p@InP-cRGD was localized after MMP2 digestion and cell uptake. Cell sensing was observed with a fluorescent microscope using 808-nm irradiation. Fluorescent emission from UCNP will transfer the energy to InP QDs and emit red fluorescence, especially in HSC4 cells (Figure 6). As expected, the HSC4 cell line with high expressions of MMP2 can be specifically sensed by UCNP-p@InP-cRGD relative to the Ca922 cell line. Integrin was highly expressed in the HSC4 cell line, whereas fluorescence was not observed in Ca922.

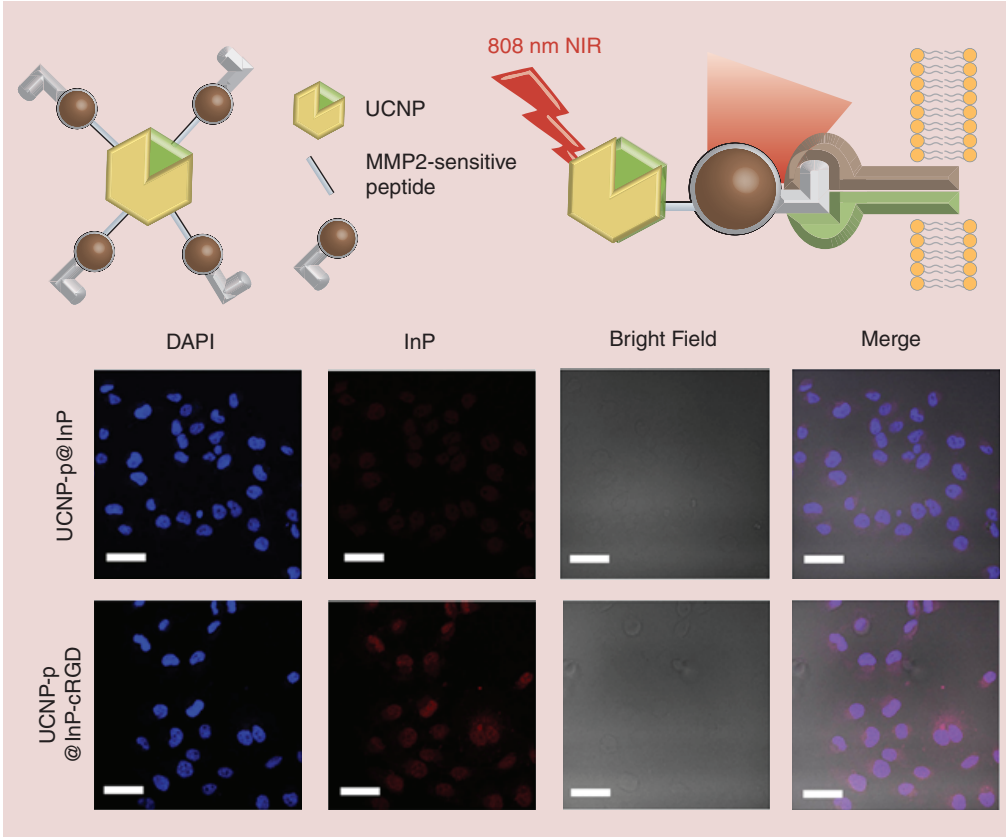

Figure 5. Detecting specific targeting ability of UCNP-p@InP-cRGD nanocomposites. Cell development of nanocomposites shows the cRGD can actively target the cancer cells and the cancer cell transfer peptide with matrix metalloproteinase-2 cells detected in the development map.
cRGD: QDs conjugated with the RGD tripeptide with chitosan; DAPI: 4′,6-Diamidino-2-phenylindole; InP: Indium phosphate; InP@S: InP and silica coating quantum dot; MMP2: Matrix metalloproteinase-2; NIR: Near-infrared radiation; UCNP: Upconversion nanoparticle; UCNP-p@InP: Upconversion nanoparticle-conjugated indium phosphide quantum dot.

In vivo visualization of mouse sensing in MMP2 overexpressing cell line

All animal works were done at Genomic Research Center, Academia Sinica, according to a protocol approved by Academia Sinica Institutional Animal Care and Utilization Committee (IACUC no. 16-05-957). We then constructed a mouse model to prove our results. The model can simulate the overexpressed MMP2 in the human body. The low MMP2-expressed cell line, Ca922 and the high MMP2-expressed cell line, HSC4 were injected in the mice's left and right thigh as a control group and experimental group. We injected the UCNP-p@InP-cRGD into the mouse through intravenous injection. The red fluorescent signal demonstrated that MMP2 expression was significantly lower in Ca922 than in HSC4 (Figure 7). Subsequently, UCNP-p@InP-cRGD was applied to HSC4 cells. The upconverting fluorescence was significantly observed in the HSC4 cell line.

Discussion

In recent years, the development of nanotechnology has received considerable attention, particularly nontoxic inorganic nanoparticles. These nanoparticles have a narrow color gamut, good biological stability and strong fluorescence intensity. These characteristics make the nanomaterials suitable to be used as biosensors [27,28]. In this work, InP QDs were chosen as effective nanoplatforms. The surface modification makes InP QDs suitable for water phase application. The size increase proves that the QDs modified with silica shell had successful single coatings. Moreover, the particle size distribution is also uniform, which proves that the dispersion of QDs is uniform. MMP2 overexpression is usually involved in local cancer cell invasion and distant metastasis, leading to poor prognosis [29]. Most tumor cells could be effectively cured by surgery at an early stage. Oral cancer usually has high lymph

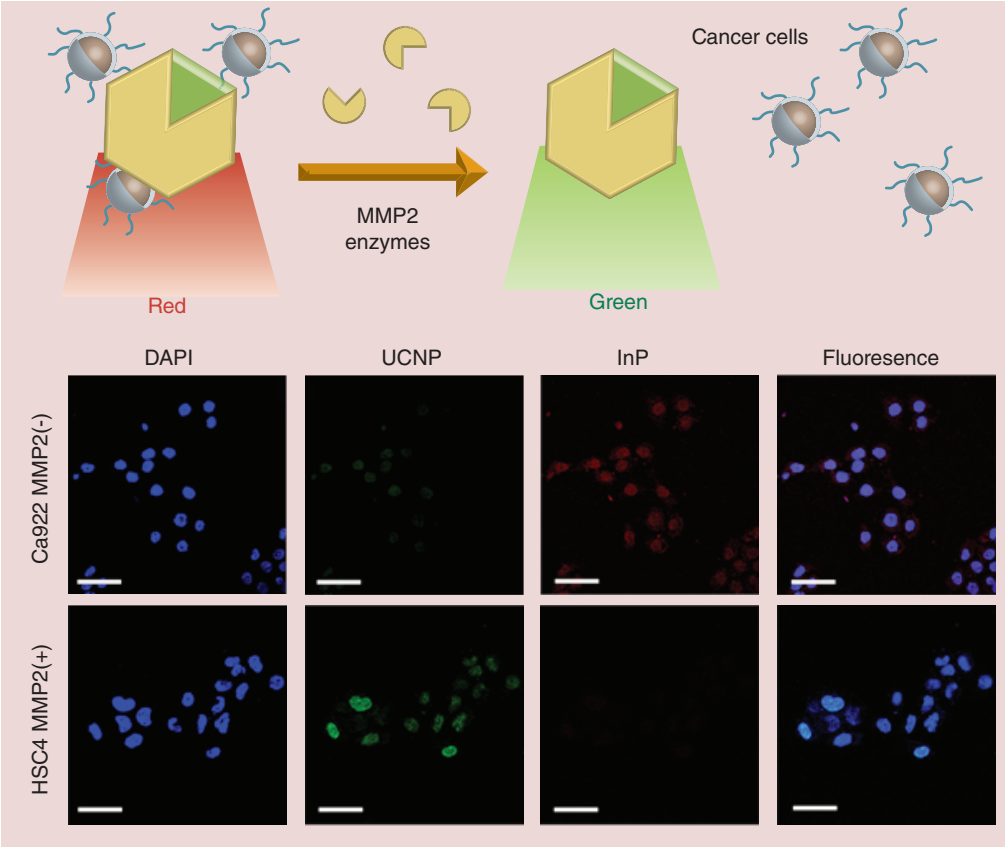

Figure 6. Ca922 and HSC4 treated with upconversion nanoparticles-p@InP-cRGD for 12 h. The treatments were processed by immunofluorescent staining and observed by fluorescence microscopy under 808-nm irradiation. DAPI: 4′,6-Diamidino-2-phenylindole; InP: Indium phosphate; MMP2: Matrix metalloproteinase-2; UCNP: Upconversion nanoparticle.

node metastasis and lacks a suitable marker for early diagnosis. Hence, we selected MMP2 to be a diagnostic 'device' in oral cancer. Based on current high research techniques, MMP2 has been detected very sensitively *in vitro*. We can even use more than two signals to enhance the acuity of MMP2 sensing and make the detection limit range of MMP2 to 0.01–10 ng/ml [30]. Following these professional studies, we hope that important cancer-related molecules such as MMP2 can be detected in real-time *in vivo*. Thus, we produced UCNP-p@InP-cRGD, a biosensor that can be recognized by MMP2. Integrin is located on the cell membrane and has high expression in cancer cells, and targeting it could help the UCNP-p@InP-cRGD nanocomposite to be close to the cell and carry out cell uptake. Several types of integrin receptors have a high affinity to RGD, especially the $\alpha_V\beta_3$ type integrin. The modification of RGD can make particles be easily accumulated in the tumor cell and enhance the signal. As a nanoscale biosensor, when MMP2 is not present in the environment, UCNPs are combined with InP QDs. At this time, if the nanocomposite is irradiated with infrared light, the upconverted energy is transmitted to the InP QDs and the InP QDs emit red light. However, when MMP2 is present in the environment, it will recognize and cut the peptide chain, causing the separation of these two nanoparticles. At this time, if we use the infrared light to excite the UCNPs, it will generate upconverted green fluorescence. As a result, the exponential dose dependence of MMP2-digested UCNP-p@InP-cRGD was between 80 and 100 pM. The sensor system was confirmed with *in vivo* cell analysis. Two different cell lines, Ca922 and HSC4, were chosen as oral cancer models. HSC4 cell line has a high degree of metastasis and performs an amount of MMP2 compared with Ca922 cell line. Thus, we suggested that MMP2 digestion did not occur in Ca922 cell sensing and only showed the InP QDs red fluorescence. This is because MMP2 protein just cut the MMP2-sensitive polypeptide from the HSC4 cells and emitted upconverted green fluorescence. Finally, we transferred the UCNP-p@InP-cRGD system into cells and mice for effect confirmation. In different concentrations of MMP2, the UCNP-p@InP-cRGD biosensor can

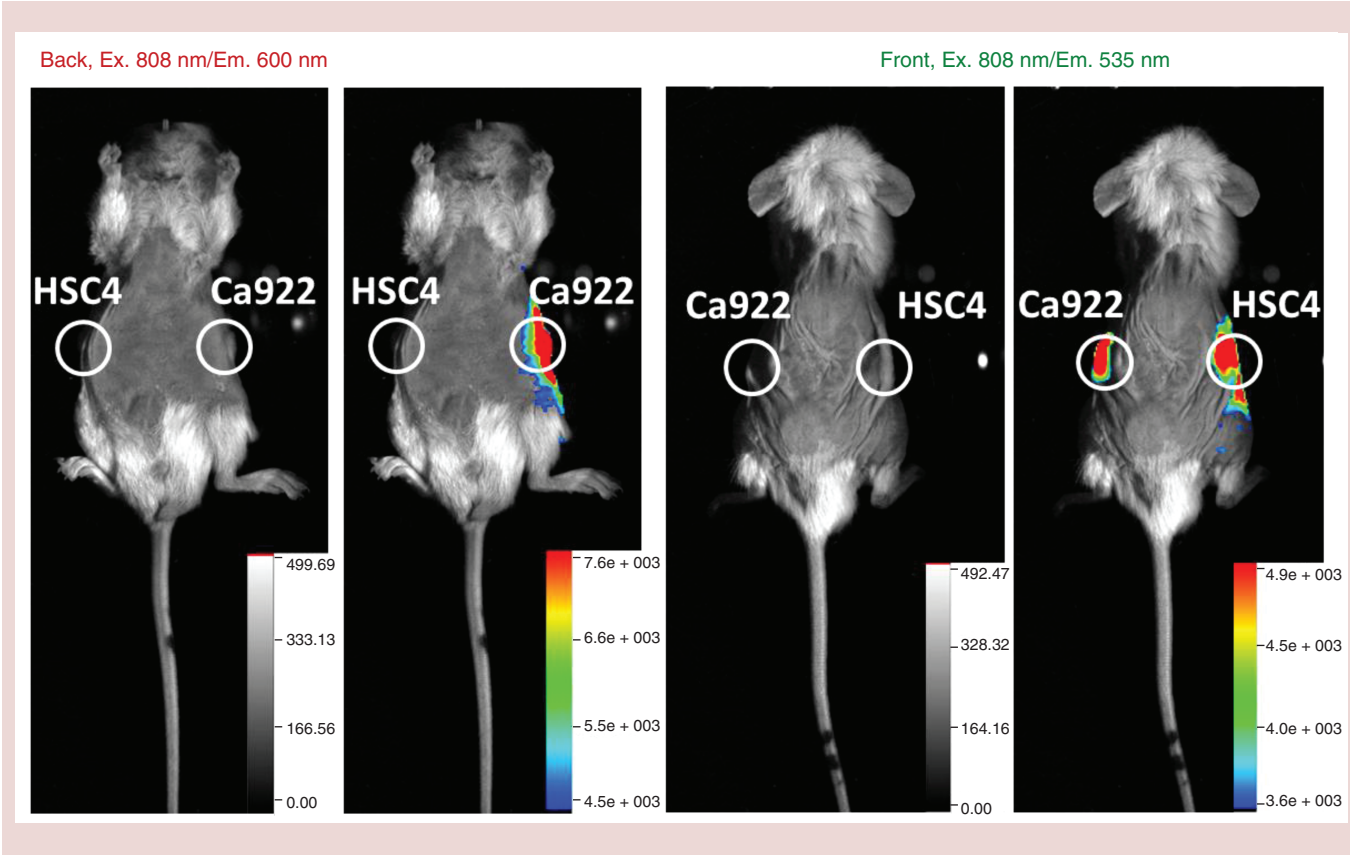

Figure 7. Matrix metalloproteinase-2 expression constructed in a matrix metalloproteinase-2-deficient cell lines Ca922 and HSC4. Composite nanoparticles combine two or more substances in a single particle. In addition to combining multiple functions, new properties of upconverting nanoparticles as a specific biosensor can also be generated.

detect the presence or absence of MMP2 by fluorescence differential specificity *in vitro* and *in vivo*. The MMP2 plays a big role in the metastatic progression of cancer cells. Current medical research usually uses blood tests to detect specific protein or molecules. This system can be tracked in the organism and the signal can be detected by the wavelength changes of the fluorescence, indicating that UCNP-p@InP-cRGD is an effective sensor. For future biomedical applications, UCNP-p@InP-cRGD can be a probe that guides MMP2 detection.

Conclusion & future perspective

In this study, we produced an MMP2-sensitive nanocomposite UCNP-p@InP-cRGD. UCNP-p@InP-cRGD can effectively detect MMP2-expressing cancer cell line (HSC4). The nanomaterial could also sense secreted MMP2 *in vitro* and *in vivo* from the cell culture during the mouse test. The MMP2 sensor can be used to detect cancers with poor prognosis induced by MMP2. The major implication of MMPs in cancer progression is their role in extracellular matrix degradation, which allows cancer cells to migrate out of the primary tumor to form metastases. Specifically, MMP-2 can degrade collagen. Degradation of the basement membrane is an essential step for metastatic progression of most cancers. This MMP2-sensitive nanocomposite can be applied to detect the amount of MMP2. Following the guides for this sensor, clinical trials for cancer therapies using MMP inhibitors may yield successful results.

Authors' contributions

All authors have given approval to the final version of the manuscript. M-H Chan, C-Y Lai and R-S Liu designed and performed the experiments and co-wrote the manuscript. Y-C Chan, M Hsiao, R-J Chung, X Chen and R-S Liu discussed the data, and developed the theoretical aspect.

Acknowledgments

The authors would like to thank CY Chien of the Precious Instrument Center (National Taiwan University) for the assistance in TEM experiments, and LW Lo and SC Hsu of Academia Sinica for their help with confocal microscopy.

Financial & competing interests disclosure

The authors would like to thank the Ministry of Science and Technology of Taiwan (Contract No. MOST 107-2113-M-002-008-MY3) to Ru-Shi Liu. The Academia Sinica (Contract No. AS-SUMMIT-108) and the Ministry of Science and Technology of Taiwan (NBA10755007-00) to Michael Hsiao for financially supporting this research. The authors have no other relevant affiliations or financial involvement with any organization or entity with a financial interest in or financial conflict with the subject matter or materials discussed in the manuscript apart from those disclosed.

Writing assistance was provided by KG Support Limited and was funded by the Ministry of Science and Technology of Taiwan (Contract No. MOST 107-2113-M-002-008-MY3).

Ethical disclosure

The authors state that they have obtained appropriate institutional review board approval or have followed the principles outlined in the Declaration of Helsinki for all animal experimental investigations. Animal works were done at Genomic Research Center, Academia Sinica, according to a protocol approved by Academia Sinica Institutional Animal Care and Utilization Committee (IACUC no. 16-05-957).

Summary points

- The development of nanotechnology received considerable attention, especially nontoxic inorganic nanoparticles.
- The indium phosphide quantum dot (InP/ZnSeS/ZnS QD) nanoparticles have a narrow color gamut, good biological stability and strong fluorescence intensity.
- In the absence of matrix metalloproteinase-2 (MMP2) in the environment, if the nanocomposite is irradiated with infrared light, then the upconverted energy is transmitted to the QDs and emit red light by the InP QDs. However, when MMP2 is present, it will recognize and cut the peptide chain, causing the separation of the two nanoparticles. Hence, if we use the infrared light to excite the upconverting nanoparticles, then it will generate upconverted green fluorescence.
- To obtain this result and determine whether MMP2 can be recognized by this biosensor, we used confocal microscopy to confirm that the nanocomposites can enter the cell via endocytosis.
- In order to facilitate the accumulation of the nanocomposite in cancer cells, the silica-coated InP QDs were modified with arginylglycylaspartic acid (RGD) molecules as targeting ligand based on chitosan, named UCNP-p@InP-cRGD. When the cell uptake images are superimposed, we found that the MMP2-based biosensor is sensitive and can be applied as a good biosensing and biotracking fluorescent probe.

References

Papers of special note have been highlighted as: • of interest; •• of considerable interest.

1. Elliott SN, Smowton PM, Krysa AB, Beanland R. The effect of strained confinement layers in InP self-assembled quantum dot material. *Semicond. Sci. Technol.* 27(9), 094008 (2012).
2. Modlitbova P, Porizka P, Novotny K *et al.* Short-term assessment of cadmium toxicity and uptake from different types of Cd-based quantum dots in the model plant Allium cepa L. *Ecotoxicol. Environ. Saf.* 153, 23–31 (2018).
3. Mason EA, Lopez R, Mason RP. Wavelength shifting of chemiluminescence using quantum dots to enhance tissue light penetration. *Opt. Mater. Express* 6(4), 1384–1392 (2016).
4. Lisenko SA, Kugeiko MM, Lisenkova AM. Noninvasive determination of spectral depth of light penetration into skin. *Opt. Spectrosc.* 115(5), 779–785 (2013).
5. Funane T, Atsumori H, Sato H, Kiguchi M, Maki A. Relationship between wavelength combination and signal-to-noise ratio in measuring hemoglobin concentrations using visible or near-infrared light. *Opt. Rev.* 16(4), 442–448 (2009).
6. Zhang JY, Chen S, Wang P *et al.* $NaYbF_4$ nanoparticles as near infrared light excited inorganic photosensitizers for deep penetration in photodynamic therapy. *Nanoscale* 9(8), 2706–2710 (2017).
7. Abdo A, Ersen A, Sahin M. Near-infrared light penetration profile in the rodent brain. *J. Biomed. Opt.* 18(7), 075001 (2013).
8. Anders JJ, Wu XJ. Comparison of light penetration of continuous wave 810 nm and superpulsed 904 nm wavelength light in anesthetized rats. *Photomed. Laser Surg.* 34(9), 418–424 (2016).

9. Ling B, Ma YH, Chen HQ, Wang L. A SPR aptamer sensor for mercury based on AuNPs@$NaYF_4$: Yb, Tm, Gd upconversion luminescent nanoparticles. *Anal. Methods* 9(42), 6032–6037 (2017).
10. Alonso-Cristobal P, Vilela P, El-Sagheer A *et al.* Highly sensitive DNA sensor based on upconversion nanoparticles and graphene oxide. *ACS Appl. Mater. Inter.* 7(23), 12422–12429 (2015).
11. Wang YD, Yang ZW, Ma YJ, Chai ZZ, Qiu JB, Song ZG. Upconversion emission enhancement mechanisms of Nd^{3+}-sensitized $NaYF_4$: Yb^{3+}, Er^{3+} nanoparticles using tunable plasmonic Au films: plasmonicinduced excitation, radiative decay rate and energy-transfer enhancement. *J. Mater. Chem. C* 5(33), 8535–8544 (2017).
12. Das K, Prasad R, Ansari SA, Roy A, Mukherjee A, Sen P. Matrix metalloproteinase-2: a key regulator in coagulation proteases mediated human breast cancer progression through autocrine signaling. *Biomed. Pharmacother.* 105, 395–406 (2018).

• **An interesting article explaining the importance of matrix metalloproteinase-2 (MMP2) molecules.**

13. Gu J, Xu FK, Zhao GY *et al.* Capn4 promotes non-small cell lung cancer progression via upregulation of matrix metalloproteinase 2. *Med. Oncol.* 32(3), 51 (2015).
14. Maatta M, Talvensaari-Mattila A, Turpeenniemi-Hujanen T, Santala M. Matrix metalloproteinase-2 (MMP-2) and-9 (MMP-9) and their tissue inhibitors (TIMP-1 and TIMP-2) in differential diagnosis between low malignant potential (LMP) and malignant ovarian tumours. *Anticancer Res.* 27(4c), 2753–2758 (2007).
15. Song EQ, Cheng D, Song Y, Jiang MD, Yu JF, Wang YY. A graphene oxide-based FRET sensor for rapid and sensitive detection of matrix metalloproteinase 2 in human serum sample. *Biosens. Bioelectron.* 47, 445–450 (2013).

• **An interesting article applying the fluorescence resonance energy transfer (FRET) of graphene oxide for MMP2 sensing.**

16. Xi GN, Wang XP, Chen TS. A reduced graphene oxide-based fluorescence resonance energy transfer sensor for highly sensitive detection of matrix metalloproteinase 2. *Int. J. Nanomedicine* 11, 1537–1547 (2016).
17. Yang GH, Li LL, Rana RK, Zhu JJ. Assembled gold nanoparticles on nitrogen-doped graphene for ultrasensitive electrochemical detection of matrix metalloproteinase-2. *Carbon* 61, 357–366 (2013).

• **An interesting article assembling the gold nanoparticles on graphene for MMP2 sensing.**

18. Wang Z, Li XH, Feng D, Li LH, Shi W, Ma HM. Poly(m-phenylenediamine)-based fluorescent nanoprobe for ultrasensitive detection of matrix metalloproteinase 2. *Anal. Chem.* 86(15), 7719–7725 (2014).
19. Montenegro CF, Casali BC, Lino RLB *et al.* Inhibition of α(v)β(3) integrin induces loss of cell directionality of oral squamous carcinoma cells (OSCC). *PLoS ONE* 12(4), e0176226 (2017).
20. Su CW, Yen CS, Chiang CS, Hsu CH, Chen SY. Multistage continuous targeting with quantitatively controlled peptides on chitosan-lipid nanoparticles with multicore-shell nanoarchitecture for enhanced orally administrated anticancer *in vitro* and *in vivo*. *Macromol. Biosci.* 17(2), 1600260 (2017).

• **An interesting article describing the targeting ability of chitosan-modified lipid and peptide.**

21. Li Q, Wen Y, You XR *et al.* Development of a reactive oxygen species (ROS)-responsive nanoplatform for targeted oral cancer therapy. *J. Mater. Chem. B* 4(27), 4675–4682 (2016).
22. Corbet C, Ragelle H, Pourcelle V *et al.* Delivery of siRNA targeting tumor metabolism using non-covalent PEGylated chitosan nanoparticles: Identification of an optimal combination of ligand structure, linker and grafting method. *J. Control. Release* 223, 53–63 (2016).
23. Jo JH, Kim JH, Lee KH *et al.* High-efficiency red electroluminescent device based on multishelled InP quantum dots. *Opt. Lett.* 41(17), 3984–3987 (2016).
24. Klier DT, Kumke MU. Upconversion luminescence properties of NaYF4:Yb:Er nanoparticles codoped with Gd^{3+}. *J. Phys. Chem. C* 119(6), 3363–3373 (2015).
25. Perera SS, Amarasinghe DK, Dissanayake KT, Rabuffetti FA. Average and local crystal structure of beta-ErYb:$NaYF_4$ upconverting nanocrystals probed by x-ray total scattering. *Chem. Mater.* 29(15), 6289–6297 (2017).
26. Kelestemur S, Altunbek M, Culha M. Influence of EDC/NHS coupling chemistry on stability and cytotoxicity of ZnO nanoparticles modified with proteins. *Appl. Surf. Sci.* 403, 455–463 (2017).
27. Chen M, Xu WM, Tian JY *et al.* A terbium(III) lanthanide-organic framework as a platform for a recyclable multi-responsive luminescent sensor. *J. Mater. Chem. C* 5(8), 2015–2021 (2017).

•• **Of considerable interest regarding the organic framework as a biosensing platform.**

28. Zhang X-J, Su F-Z, Chen D-M *et al.* A water-stable EuIII-based MOF as a dual-emission luminescent sensor for discriminative detection of nitroaromatic pollutants. *Dalton Trans.* 48(5), 1843–1849 (2019).

•• **Of considerable interest regarding the metal organic frameworks as a biosensing platform.**

29. Chan YC, Chen CW, Chan MH *et al.* MMP2-sensing up-conversion nanoparticle for fluorescence biosensing in head and neck cancer cells. *Biosens. Bioelectron.* 80, 131–139 (2016).

•• **Of considerable interest regarding the MMP2-sensing inorganic nanocomposites.**

30. Wang HQ, Ma ZF. A novel strategy for improving amperometric biosensor sensitivity using dual-signal synergistic effect for ultrasensitive detection of matrix metalloproteinase-2. *Sensor Actuat. B Chem.* 266, 46–51 (2018).